Detection of a very rapid first phase in complex formation of DnaK and peptide substrate

Michael F. Koller, Antonio Baici, Michael Huber, Philipp Christen*

Biochemisches Institut der Universität Zürich, Winterthurerstrasse 190, CH-8057 Zürich, Switzerland

Received 28 March 2002; revised 8 April 2002; accepted 9 April 2002

First published online 29 April 2002

Edited by Thomas L. James

Abstract Complex formation of the Hsp70 chaperone DnaK with the fluorescence-labeled peptide ALLLSAPRR shows a very rapid first phase that has as yet not been observed with other peptides. This first phase is completed within the dead time (1–2 ms) of the stopped-flow instrument and corresponds to two thirds of the total increase in fluorescence. It occurs both in the presence and in the absence of ATP and is followed by a fast, a slow and a very slow step. These binding kinetics that are vastly different from those observed with other peptides might indicate the existence of a second substrate-binding site of DnaK. © **2002 Federation of European Biochemical Societies. Published by Elsevier Science B.V. All rights reserved.**

Key words: Molecular chaperone; Hsp70; DnaK; Kinetics of Hsp70; Stopped-flow technique; Fluorescence-labeled peptide

1. Introduction

DnaK is a 70-kDa heat shock protein (Hsp70) homolog of *Escherichia coli*. An important function of Hsp70 chaperones is to facilitate the correct folding of nascent and denatured proteins (for a review, see [1]). DnaK consists of a highly conserved NH_2-terminal ATPase domain with a mass of 44 kDa, followed by the 27-kDa substrate-binding domain [2–4]. DnaK has been found to bind preferentially peptides with a hydrophobic core of four to five residues containing in particular leucine, but also isoleucine, valine, phenylalanine or tyrosine residues, and flanking regions of basic residues. Negatively charged peptides are bound with low affinity [5,6]. Hsp70 chaperones also bind unfolded proteins such as bovine pancreatic trypsin inhibitor, RNA polymerase, reduced carboxymethylated α-lactalbumin, rhodanese [7], and native proteins like λP, λO [8], RepA [9], p53 [10], σ^{32} [11] and apocytochrome *c* [12]. ATP-liganded (T state) DnaK binds substrates with low affinity and fast on and off rates, ADP-liganded and nucleotide-free (R state) DnaK shows high affinity and slow on and off rates [13–15]. DnaK acts in concert with its co-chaperones DnaJ and GrpE. DnaJ, an Hsp40 homolog of *E. coli*, stimulates the hydrolysis of DnaK-bound ATP, initiating the conversion of DnaK from the T to the R state; GrpE facilitates ADP/ATP exchange and thus the switch from the R state back to the T state.

Fluorescence-labeled peptide substrates [14,16,17] have been used to determine the kinetics of the formation of DnaK–peptide complexes. Complex formation was reported to be a single- or double-exponential process and to occur at different rates [18], depending on the structure of the peptide. Here, we compared complex formation of peptide ala-p5 (ALLLSAPRR), labeled at its α-amino group with fluorescent acrylodan, with that of acrylodan-labeled NR peptide (NRLLLTG). Both in the presence and in the absence of ATP, peptide a-ala-p5 showed, in contrast to a-NR, a very rapid first phase, which was finished within the dead time of the stopped-flow instrument, followed by three slower phases.

2. Materials and methods

2.1. Materials

Peptide NR (NRLLLTG) was purchased from Chiron, Australia (purity >80%) and ala-p5 (ALLLSAPRR) was synthesized by Dr. S. Klauser of our Institute using the orthogonal Fmoc protection strategy with an ABI 430 A peptide synthesizer (Applied Biosystems). 6-Acryloyl-2-dimethylaminonaphthalene (acrylodan) was from Molecular Probes (Eugene, OR, USA) and ATP disodium salt hydrate (purity >98%) from Fluka (Switzerland). The peptides were labeled at their α-amino group with acrylodan as described [14,19].

2.2. Expression and purification of wild-type DnaK

The plasmid pTPG9 was inserted into *dnak*-deficient *E. coli* BB1553 cells [20]. After induction with isopropyl-β-D-thiogalactopyranoside, DnaK was isolated as described [14] and stored at −80°C in 25 mM Tris–HCl, 10 mM 2-mercaptoethanol, 1 mM EDTA, 5% glycerol, pH 8.0. The concentration of DnaK was determined photometrically with a molar absorption coefficient of $\varepsilon_{280} = 14500\ M^{-1}\ cm^{-1}$ [21]. The last step in the purification procedure was a size-exclusion chromatography in the absence of KCl which decreases the nucleotide content to <0.1 mol/mol DnaK [22]. Molecular mass and purity of DnaK were verified by mass spectroscopy and SDS–PAGE with silver staining, respectively.

2.3. Kinetic measurements

2.3.1. Practical aspects. All experiments were performed in assay buffer (25 mM HEPES, 100 mM KCl, 5 mM $MgCl_2$, pH 7.0) at 25°C in the presence or absence of 1 mM ATP. The kinetics of association between peptides a-ala-p5 or a-NR and wild-type DnaK were measured with a SF-61 stopped-flow spectrofluorimeter (HiTech Scientific, Salisbury, UK) having a dead time of 1–2 ms. The reactions were started by mixing equal volumes (60 μl each) of the reactants. To assure pseudo-first-order conditions, the final concentration of the labeled peptide was kept constant at 200 nM and that of DnaK was varied between 1.25 and 20 μM. The course of the reaction was followed in logarithmic time mode, the method of choice for collecting

*Corresponding author. Fax: (41)-1-6355907.
E-mail address: christen@bioc.unizh.ch (P. Christen).

Abbreviations: a-ala-p5, acrylodan-labeled peptide ala-p5 (ALLLSAPRR); a-NR, acrylodan-labeled peptide NR (NRLLLTG); Hsc70, 70-kDa heat shock cognate protein; Hsp70, 70-kDa heat shock protein

PII: S0014-5793(02)02752-7

data of multiexponential processes, which also facilitates non-linear regression analysis [23]. To prevent loss of data in fast reactions, the time constant of the stopped-flow apparatus was kept at 0.33 ms. The fluorescence emission of the acrylodan-labeled peptide was monitored with excitation at 370 nm (band-pass 12 nm) and passing the emitted light through a GG455 cut-off filter. The temperature of 25 ± 1°C was controlled with a circulating thermostat. Fitting of equations to data was performed with Prism 3 (GraphPad) and SigmaPlot 5 (SPSS) software.

2.3.2. Theory. The kinetic profiles for complex formation of a-ala-p5 and wild-type DnaK were characterized by an unmeasurably fast first phase followed by three measurable exponential phases. The very fast step was completed within the dead time of the stopped-flow instrument. The general kinetic scheme, which may be applied to this system, is a four-step linear mechanism, in which the product of one reaction is the reactant for the next reaction:

$$A + B \underset{k_{-1}}{\overset{1\ k_1}{\rightleftharpoons}} X_1 \underset{k_{-2}}{\overset{2\ k_2}{\rightleftharpoons}} X_2 \underset{k_{-3}}{\overset{3\ k_3}{\rightleftharpoons}} X_3 \underset{k_{-4}}{\overset{4\ k_4}{\rightleftharpoons}} X_4 \quad (1)$$

In Eq. 1, A represents a-ala-p5, B represents DnaK, and X_1 to X_4 denote chaperone–peptide complexes. The numbers above the kinetic constants indicate the four equilibria. The treatment of Castellan [24] and its elaboration by Hammes and Schimmel [25,26] facilitate the derivation of the expressions for the reciprocal relaxation times of this mechanism. Briefly, the four reciprocal relaxation times in mechanism 1, i.e. $1/\tau_1$, $1/\tau_2$, $1/\tau_3$ and $1/\tau_4$, correspond to the eigenvalues of the secular determinant:

$$\begin{vmatrix} k' + k_{-1}{}^{-1}/\tau & -k_{-1} & 0 & 0 \\ -k_2 & k_2 + k_{-2}{}^{-1}/\tau & -k_{-2} & 0 \\ 0 & -k_3 & k_3 + k_{-3}{}^{-1}/\tau & -k_{-3} \\ 0 & 0 & -k_4 & k_4 + k_{-4}{}^{-1}/\tau \end{vmatrix} = 0 \quad (2)$$

In this determinant, $k'_1 = k_1(\bar{c}_A + \bar{c}_B)$, where $\bar{c}_A$ and $\bar{c}_B$ are the equilibrium concentrations of the reactants. The mathematical treatment of Hammes and Schimmel [25] provides analytical representations of the four reciprocal relaxation times, the expressions of which depend on the relative rates of equilibration of the four steps in mechanism 1. The indices of the relaxation times, τ_1 through τ_4, indicate relative rates, with τ_1 being the shortest and τ_4 the longest relaxation time [27]. Depending on the particular situation, a relaxation time may contain the rate constants of just one step, or all eight rate constants of the system (for a summary of three particular cases of mechanism 1, see Table 1).

In the case of complex formation of DnaK with peptide a-NR the kinetic profiles in the absence and presence of ATP were characterized by two and three exponential phases, respectively. The general kinetic scheme, which may be applied to this system, is again a linear mechanism, in which the product of one reaction is the reactant for the following reaction. The mathematical treatment for two- and three-step mechanisms is of the same type as outlined above. The mathematical analysis of a two-step linear mechanism has been described elsewhere [28]. Further details are explained in Section 3.

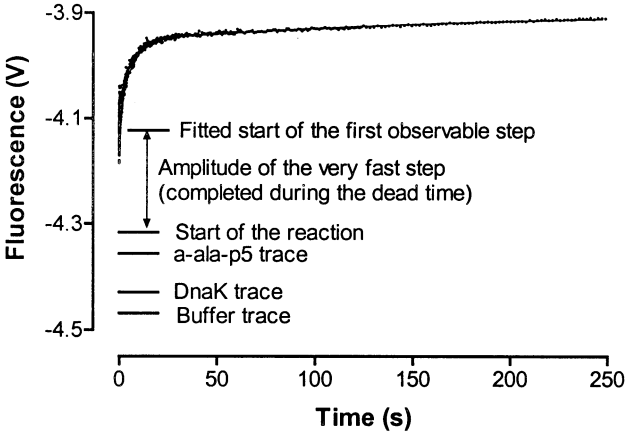

Fig. 1. Kinetic profile of complex formation of wild-type DnaK with a-ala-p5 in the absence of ATP. After mixing in a stopped-flow device, the final concentrations of a-ala-p5 and DnaK were 200 nM and 10 μM, respectively. For details of the stopped-flow experiments, see Section 2. The starting point of the reaction was calculated by adding the contributions of the free peptide and of DnaK to the buffer trace. A triple exponential equation was fitted to the curve, which was collected in logarithmic time mode and was averaged from three measurements.

3. Results

3.1. Binding of peptide a-ala-p5 to DnaK

The mechanism of complex formation of DnaK with a-ala-p5 was investigated by the stopped-flow technique. Measurement of the zero-time fluorescence intensity showed that in the case of a-ala-p5 the recorded reaction traces started at considerably higher fluorescence values (Fig. 1). The traces corresponding to buffer alone, labeled peptide alone (at a fixed final concentration of 200 nM in all experiments), and DnaK alone (at final concentrations of 1.25, 2.5, 5.0, 10.0, and 20.0 μM) were measured for each series of experiments. The small contribution of DnaK to the fluorescence signal was concentration-dependent, and was likely due to light scattering. The starting point of the reaction was obtained by adding the signals of the labeled peptide and of DnaK to the buffer trace. The noise of the reaction traces for the association of peptide and DnaK was relatively large at the beginning of the reaction and then decreased progressively (Figs. 1 and 2). This feature is characteristic for the logarithmic time capture mode. The starting point of the first observable step was obtained by curve fitting (Fig. 1). The difference in fluorescence intensity between this fitted starting point of the first observable reac-

Table 1
Reciprocal relaxation times for different rate sequences of a four-step linear mechanism[a]

	1 very fast 3 slow	2 fast 4 very slow	1 very fast 3 fast	2 slow 4 very slow	1 very fast 3 fast	2 very slow 4 slow
$1/\tau_1$	k'_1+k_{-1}		k'_1+k_{-1}		k'_1+k_{-1}	
$1/\tau_2$	$k_2\frac{K'_1}{1+K'_1}+k_{-2}$		k_3+k_{-3}		k_3+k_{-3}	
$1/\tau_3$	$k_3\frac{K'_1K_2}{1+K'_1+K'_1K_2}+k_{-3}$		$k_{-2}\frac{1}{1+K_3}+k_2\frac{K'_1}{1+K'_1}$		$k_4\frac{K_3}{1+K_3}+k_{-4}$	
$1/\tau_4$	$k_4\frac{K'_1K_2K_3}{1+K'_1+K'_1K_2+K'_1K_2K_3}+k_{-4}$		$k_4\frac{K'_1K_2K_3}{1+K'_1+K'_1K_2+K'_1K_2K_3}+k_{-4}$		$k_{-2}\frac{1}{1+K_3+K_3K_4}+k_2\frac{K'_1}{1+K'_1}$	

[a]The numbers and the relative rates of equilibration in the first row refer to the equilibria in mechanism 1.
$k'_1 = k_1(\bar{c}_A+\bar{c}_B)$, $K_i = k_i/k_{-i}$, $K'_1 = K_1(\bar{c}_A+\bar{c}_B)$.

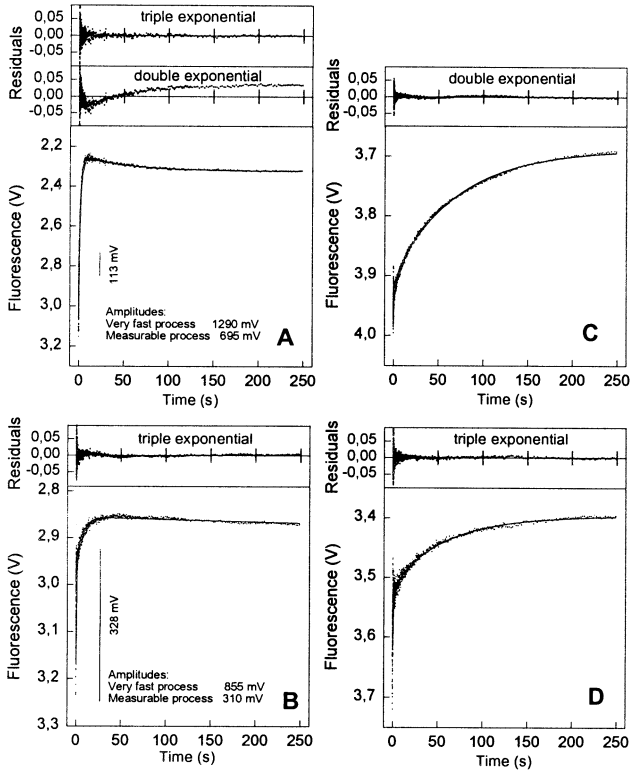

Fig. 2. Kinetic course of complex formation between peptide and DnaK. In all panels, the concentrations of peptide and chaperone were 200 nM and 20 μM, respectively. A: a-ala-p5+DnaK. B: a-ala-p5+DnaK in the presence of 1 mM ATP. C: a-NR+DnaK. D: a-NR+DnaK in the presence of 1 mM ATP. The curves represent the average of at least three measurements. A triple-exponential function was necessary to describe the a-ala-p5 association, as shown by the residuals analysis on the top of each panel. In A, the worse fitting produced by a double-exponential function is shown. The calculated amplitudes (in mV) of the very fast phase preceding the first measurable relaxation as well as the amplitude of the measurable process are indicated. The vertical, labeled bars represent the fluorescence of 200 nM a-ala-p5 in assay buffer as an internal standard. The a-NR associations were described by a double-exponential function and a triple-exponential function in the absence and the presence of ATP, respectively. The fluorescence of 200 nM a-NR in assay buffer was 521 mV and 996 mV for C and D, respectively.

tion and the calculated starting point of the overall reaction indicates the existence of a first reaction phase with a relaxation time shorter than the dead time of the stopped-flow device (1–2 ms). This very rapid phase occurs both in the absence and in the presence of ATP and has as yet not been described for Hsp70 chaperones.

The kinetic profiles of complex formation showed three measurable exponential phases following the very fast first reaction phase (Fig. 2A,B). A double-exponential function resulted in worse fitting (Fig. 2A). The association of wild-type DnaK and a-ala-p5 was faster in the presence of ATP (Fig. 2B, Table 2), the fastest measurable process (20 μM DnaK, 200 nM of a-ala-p5 in the presence of ATP; Fig. 2B) having a half-life of 27 ms.

The amplitude of the first, very fast step (Fig. 2) deserves some attention for its impact on the kinetic mechanism of chaperone–peptide association. Considering the overall reaction amplitude as the sum of the amplitudes of the very fast first phase and of the measurable phases, the amplitude of the very fast phase contributed 65% and 73% in the absence and presence of ATP, respectively (Fig. 2A,B).

We conclude that the very fast relaxation observed at the beginning of the reaction is kinetically relevant and must be considered in formulating a mechanism and in calculating the rate constants. In fact, all plots of $1/\tau_2$ and $1/\tau_3$ as a function of DnaK concentration were hyperbolic (Fig. 3). The hyperbolic dependence of the first observable relaxation (τ_2) on DnaK concentration implies the existence of a much faster relaxation (τ_1) preceding it [27]. The fact that the third relaxation (τ_3) was also hyperbolically dependent on concentration strongly points to a sequential mechanism according to Eq. 1, characterized by the reciprocal relaxation times shown in Table 2 for the sequence of four steps with the relative equilibration rates being very fast, fast, slow, and very slow (Table 1, first column).

If all relaxation times of mechanism 1 could be measured, all kinetic constants could be calculated [29]. In the particular case analyzed here, the first relaxation (τ_1) was too fast to be measured, and the slowest relaxation (τ_4) was affected by large standard errors of the parameters calculated by non-linear regression analysis. Thus, not all kinetic constants could be evaluated. Though the hyperbolae in Fig. 3 were highly diag-

Table 2
Rate and equilibrium constants for complex formation of DnaK and peptide[a]

	a-ala-p5		a-NR	
	Without ATP	With ATP	Without ATP	With ATP
k_1 (M^{-1} s^{-1})	Not measurable	Not measurable	$6.6 \pm 1.1 \times 10^3$	$4.10 \pm 0.24 \times 10^5$
k_{-1} (s^{-1})	Not measurable	Not measurable	$6.1 \pm 1.3 \times 10^{-2}$	
K_1 (M^{-1})	$7.5 \pm 2.1 \times 10^4$	$1.3 \pm 0.4 \times 10^5$	$1.1 \pm 0.3 \times 10^5$	1×10^6
k_2 (s^{-1})	6.7 ± 0.7	33 ± 2	$1.8 \pm 0.3 \times 10^{-2}$	0.1
k_{-2} (s^{-1})	0.44 ± 0.19	≤ 0.2	$1.9 \pm 1.7 \times 10^{-3}$	
K_2	15.2 ± 6.7	≥ 165	9.5 ± 8.6	
k_3 (s^{-1})	0.25	0.28	–	
k_{-3} (s^{-1})	0.011 ± 0.003		–	
K_3	25.4		–	

[a]The values given are calculated from the experiments shown in Figs. 2 and 3. Numbers after a ± sign indicate the S.E.M. from regression analysis. The S.E.M. of a quotient Q (e.g. k_i/k_{-i}) of two parameters $A \pm a$ and $B \pm b$, with a and b representing S.E.M., was calculated according to Fenner [32]:

$$Q \pm q = \frac{A \pm a}{B \pm b} = \frac{A}{B} \pm \frac{1}{B^2}\sqrt{B^2a^2 + A^2b^2}$$

Numbers not accompanied by an S.E.M. represent estimates from cross-calculations using the plots of $1/\tau_2$ and $1/\tau_3$ versus concentration. Void spaces indicate parameters that cannot be determined reliably on the basis of the present data.

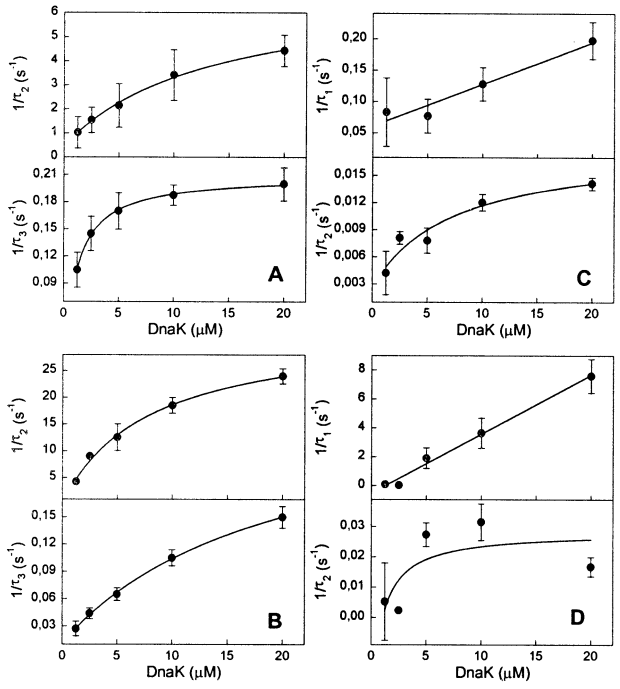

Fig. 3. Dependence of the reciprocal relaxation times on the concentration of the chaperone. The concentration of DnaK was varied from 1.25 μM to 20 μM. A: a-ala-p5+DnaK. B: a-ala-p5+DnaK in the presence of 1 mM ATP. C: a-NR+DnaK. D: a-NR+DnaK in the presence of 1 mM ATP. The primary data were obtained from multi-exponential non-linear regression analysis of reaction traces as shown in Fig. 2. Experimental points were fitted linearly or with the equation of a rectangular hyperbola with intercept on the ordinate. The corresponding plots for $1/\tau_4$ in the a-ala-p5/DnaK system, which contained large standard errors of the observed reciprocal relaxation times, were not used for computations and are not shown. In some cases, the very small amplitudes at low chaperone concentrations were barely observable. However, the inclusion of relaxation time τ_4 was necessary for curve fitting to avoid a bias in the determination of $1/\tau_2$ and $1/\tau_3$. The same applies for the $1/\tau_3$ plot in the a-NR/DnaK/ATP system.

nostic for the mechanism, the parameters could not be calculated with sufficient precision in all cases, in particular the constants k_{-2} and k_{-3}, which were obtained as intercepts on the ordinate. When the curve extrapolates very closely to the origin, the two parameters are undetermined. However, cross-computations between the two plots ($1/\tau_2$ and $1/\tau_3$ versus concentration) allowed an estimate of some parameters (Table 2).

3.2. Binding of peptide a-NR to DnaK

Complex formation of a-NR with DnaK showed two measurable exponential phases in the absence of ATP and three phases in the presence of ATP (Fig. 2C,D). As there was no jump between the baseline and the beginning of the measured curve and as $1/\tau_1$ and $1/\tau_2$ increased linearly and hyperbolically, respectively, with increasing concentration of DnaK (Fig. 3C,D), a very fast phase preceding the measurable steps – as in the case of a-ala-p5 – could be excluded [28]. The kinetic parameters (Table 2) were calculated, if possible, from reaction traces as shown in Fig. 2C,D using the first column of Table 1 because each step was faster than the following one.

4. Discussion

The very rapid first phase of complex formation between DnaK and fluorescence-labeled peptide a-ala-p5 is completed within the dead time of stopped-flow instruments (1–2 ms) and has as yet eluded detection. The very rapid first phase is followed by three slower phases. This kinetic mechanism, however, does not apply to all peptides, e.g. it was not observed with a-NR and numerous other peptides used in previous studies [17,18]. The kinetic traces obtained with a-NR in the absence of ATP can be fitted double-exponentially and triple-exponentially in the presence of ATP. A very fast phase preceding the other two or three measurable phases can be excluded because the measurable reaction starts directly at the baseline without a jump and the mathematical analysis of the kinetic data (Fig. 3C,D) agrees with the first measurable phase not being preceded by another phase. In all investigated cases, i.e. with both peptide a-ala-p5 and a-NR and both in the absence and in the presence of ATP, each step is faster than the following one. K_1, the equilibrium constant of the first step in complex formation, should not be mistaken for the overall association equilibrium constant which cannot be determined from our data. Only in one case, i.e. a-NR in the absence of ATP, the overall K_d could be calculated; the value of 1 μM corresponds well with the value of 0.5 μM determined by titration (M.F. Koller, M. Huber, A. Baici, N.B. König, T. Grau, P. Bischofberger, H.-J. Schönfeld and P. Christen, in preparation).

The very rapid first phase observed with a-ala-p5 is not an artefact merely due to binding of the fluorophore since acrylodan-labeled 2-mercaptoethanol does not react with DnaK (not shown). The unmeasurable first phase has an amplitude exceeding the sum of the following three observable phases. In this study, the concentrations of the peptide substrate was four-fold higher than in earlier experiments [14,16–18]. The correspondingly higher fluorescence signal might explain why two or three measurable phases were observed instead of the only one or two phases in the earlier experiments.

The mechanistic significance of the differential kinetics of the two peptides is open to conjecture. Peptide ala-p5 (ALLLSAPRR) is a deviation of the prepiece of imported mitochondrial aspartate aminotransferase [14] while peptide NR (NRLLLTG) was identified as a good binder to DnaK by screening a phage-displayed peptide library [30]. Conspicuous features of peptide ala-p5 are the proline and the two arginine residues at its COOH-terminus. A plausible interpretation of the deviant kinetic behavior is that this peptide binds to an alternative binding site. The existence of a binding site other than the hydrophobic peptide-binding cleft was recently also postulated for a peptide (NIVRKKK) that with its strong positive charge at the COOH-terminus is quite similar in structure to peptide ala-p5 [31]. Possibly, the combination of a hydrophobic NH_2-terminus with multiple positively charged amino acid residues at the COOH-terminus targets peptides to the second binding site.

Acknowledgements: This work was supported by Swiss National Science Foundation Grant 31-51881.97. The costs of publication of this article were defrayed in part by the payment of page charges. This article must therefore be hereby marked 'advertisement' in accordance with 18 U.S.C. Section 1734 solely to indicate this fact.

References

[1] Bukau, B. and Horwich, A.L. (1998) Cell 92, 351–366.
[2] Wang, T.F., Chang, J.H. and Wang, C. (1993) J. Biol. Chem. 268, 26049–26051.
[3] Zhu, X., Zhao, X., Burkholder, W.F., Gragerov, A., Ogata, C.M., Gottesman, M.E. and Hendrickson, W.A. (1996) Science 272, 1606–1614.
[4] Harrison, J.C., Hayer-Hartl, M., Di Liberto, M., Hartl, F.U. and Kuriyan, J. (1997) Science 276, 431–435.
[5] Rüdiger, S., Germeroth, L., Schneider-Mergener, J. and Bukau, B. (1997) EMBO J. 16, 1501–1507.
[6] Kasper, P., Christen, P. and Gehring, H. (2000) Proteins 40, 185–192.
[7] Hendrick, J.P. and Hartl, F.U. (1993) Annu. Rev. Biochem. 62, 349–384.
[8] Liberek, K., Osipiuk, J., Zylicz, M., Ang, D., Skorko, J. and Georgopoulos, C. (1990) J. Biol. Chem. 265, 3022–3029.
[9] Wawrzynow, A. and Zylicz, M. (1995) J. Biol. Chem. 270, 19300–19306.
[10] Hupp, T.R., Meek, D.W., Midgley, C.A. and Lane, D.P. (1992) Cell 71, 875–886.
[11] Liberek, K., Galitski, T.P., Zylicz, M. and Georgopoulos, C. (1992) Proc. Natl. Acad. Sci. USA 89, 3516–3520.
[12] Sadis, S. and Hightower, L.E. (1992) Biochemistry 31, 9406–9412.
[13] Palleros, D.R., Reid, K.L., Shi, L., Welch, W.J. and Fink, A.L. (1993) Nature 365, 664–666.
[14] Schmid, D., Baici, A., Gehring, H. and Christen, P. (1994) Science 263, 971–973.
[15] Pierpaoli, E.V., Sandmeier, E., Baici, A., Schönfeld, H.J., Gisler, S. and Christen, P. (1997) J. Mol. Biol. 269, 757–768.
[16] Gisler, S.M., Pierpaoli, E.V. and Christen, P. (1998) J. Mol. Biol. 279, 833–840.
[17] Witt, S.N. and Slepenkov, S.V. (1999) J. Fluoresc. 9, 281–293.
[18] Pierpaoli, E.V., Gisler, S.M. and Christen, P. (1998) Biochemistry 37, 16741–16748.
[19] Pierpaoli, E.V., Sandmeier, E., Schönfeld, H.J. and Christen, P. (1998) J. Biol. Chem. 273, 6643–6649.
[20] Bukau, B. and Walker, G.C. (1990) EMBO J. 9, 4027–4036.
[21] Hellebust, H., Uhlen, M. and Enfors, S.O. (1990) J. Bacteriol. 172, 5030–5034.
[22] Feifel, B., Sandmeier, E., Schönfeld, H.J. and Christen, P. (1996) Eur. J. Biochem. 237, 318–321.
[23] Walmsley, A.R. and Bagshaw, C.R. (1989) Anal. Biochem. 176, 313–318.
[24] Castellan, G.W. (1963) Ber. Bunsenges. Phys. Chem. 67, 898–908.
[25] Hammes, G.G. and Schimmel, P.R. (1966) J. Phys. Chem. 70, 2319–2324.
[26] Hammes, G.G. and Schimmel, P.R. (1967) J. Phys. Chem. 71, 917–923.
[27] Bernasconi, C.F. (1976) Relaxation Kinetics, Academic Press, New York, Chapter 4.
[28] Hiromi, K. (1979) Kinetics of Fast Enzyme Reactions, John Wiley and Sons, New York, pp. 195–220.
[29] Haslam, J.L. (1972) J. Phys. Chem. 76, 366–369.
[30] Gragerov, A., Zeng, L., Zhao, X., Burkholder, W. and Gottesman, M.E. (1994) J. Mol. Biol. 235, 848–854.
[31] Thulasiraman, V., Yun, B.G., Uma, S., Gu, Y., Scroggins, B.T. and Matts, R.L. (2002) Biochemistry 41, 3742–3753.
[32] Fenner, G. (1931) Naturwissenschaften 19, 310.